Highly Isolated Y-shape Two-Port THz Antenna Based on Hybrid Decoupling Structure

Praveen Kumar
Department of Electronics and Communication Engineering, Manipal Institute of Technology, Manipal Academy of Higher Education, Manipal 576104, India
pkonda57@gmail.com

Tanweer Ali
Department of Electronics and Communication Engineering, Manipal Institute of Technology, Manipal Academy of Higher Education, Manipal 576104, India
tanweer.ali@manipal.edu

Manohara Pai M M
Department of Information and Communication Technology, Manipal Institute of Technology, Manipal Academy of Higher Education, Manipal 576104, India
mmm.pai@manipal.edu

***Abstract*— The fascinating properties of terahertz (THz) waves piqued the interest of numerous researchers in THz technology. This paper introduces a Y-shaped two-port THz antenna operating from 0.87-1.9 THz. The proposed THz MIMO antenna has an overall geometry of 600×1400×20 µm^3. The proposed THz MIMO antenna is designed on a 20 µm thick polyimide substrate with a relative permittivity of 3.5. To realize the appropriate operating frequency and isolation antenna's radiator and ground plane are adjusted by integrating parasitic elements. The isolation among the inter port of the antenna is enhanced to better than 22 dB using a hybrid decoupling structure comprised of a neutralization line and defected ground structure. MIMO diversity features of the proposed antenna are examined and found to be ECC <0.001, DG≈ 10 dB, TARC <-10 dB, CCL<0.2 bps/Hz, and MEG<-3 dB across the impedance bandwidth of the antenna. The diversity parameters result ensures that the proposed MIMO design is well suited for wireless communication applications.**

Keywords*— *THz antenna, MIMO, Hybrid decoupling, Isolation, DGS, NL

I. INTRODUCTION

Data traffic is increasing exponentially in wireless communication networks over time. Due to the increase in mobile phone users, ongoing use of multimedia, the Internet of Things, and effects on mobile network services, this trend is anticipated to grow in the coming days [1]. The terahertz (THz) frequency, used in developing silicon-based integrated system technologies, attracts spectrum frequencies with wavelengths between 30 µm and 3 mm between the microwave and infrared frequency range [2–3]. The developing THz frequency spectrum will be an option for applications requiring huge bandwidths. Terahertz waves have several benefits, including a low ionizing effect, high spectral resolution and visibility, penetrating non-metal materials, sensing, imaging, biological and medical applications, and ultra-high-speed wireless communications [4-9]. THz communications are rapidly being highlighted as an intriguing possibility to the upcoming bandwidth restriction since THz systems offer the potential capability of many terabits per second [4]. THz devices are also robust to adverse environmental circumstances [6]. However, developing an antenna with scalable, larger impedance bandwidth, cost-efficient, and easy integration with the transceiver is complicated regarding THz wireless communication application. On the contrary, to give the user a seamless experience, the current wireless system necessitates a high data rate and channel capacity. To suit the requirements of the wireless system, the single-element antenna needs to be transformed into multiple input and multiple output (MIMO) antennas. When antennas are arranged with a spacing of less than a quarter wavelength to achieve compactness, the inevitable issue of mutual coupling of the MIMO antenna develops. Various ways to design the THZ MIMO antenna with increased isolation are presented in the literature.

A two-port circular patch antenna with the defected ground structure (DGS) to enhance the isolation among the inert elements is presented in [10]. The THz MIMO antenna has a geometry of 1000×1400 µm^2 operating in the frequency range of 0.33-10 THz. The rectangular THz antenna is configured in the orthogonal arrangement to achieve the reduced mutual coupling with the dimension of 135×80 µm^2 [11]. A 90×170 µm^2 modified rectangular THz antenna is orthogonally arranged by incorporating the metamaterial (MTM) loading to enhance the isolation presented in [12]. An inset feed rectangular patch antenna with metamaterial surface loading is presented in [13]. The proposed arrangement has a total geometry of 188×160 µm^2 and impedance bandwidth from 1.281-1.354 THz. The rectangular patch THz MIMO antenna is designed by creating elliptical slots onto the radiator to decrease the mutual coupling with the overall size of 150×100 µm^2, as shown in [14]. The improvement in the bandwidth and gain is achieved by loading the nested rectangular ring MTM surface onto the antenna's radiator. The rectangular slotted inset feed antenna using hard rubber as substrate operating at the 0.1 THz, having a physical size of 900×700 µm^2, is proposed in [15]. The majority of THz MIMO designs accessible in the literature are traditional rectangular or circular patch antennas and use orthogonal configuration, MTM loading, and DGS as a decoupling structure to improve isolation among the MIMO antenna system's inter ports.

This work describes a distinctive two-port modified Y-shaped patch antenna operating in the 0.87-1.9 THz frequency band. The hybrid decoupling structure, which consists of a neutralization line and DGS, improves the isolation among the

MIMO antenna's inter ports. This hybrid decoupling arrangement provides isolation of more than 22 dB over the antenna's impedance bandwidth. Further, the proposed antenna's radiation properties and MIMO diversity features were investigated. The remainder of the paper is structured as follows: antenna design methodology is depicted in section 2. Section 3 presents the research findings regarding S-parameters, radiation characteristics, and diversity features. Concluding remarks are presented in section 4.

II. Antenna Design Methodology

The conventional rectangular monopole antenna is modified by incorporating multiple curved segments onto the radiator and reduced ground plane to realize the antenna to be operated in the THz frequency range. The modification of the antenna structure alters the transmission line properties and quality factor and helps realize the desired THz frequency. The modified Y-shaped THz antenna is parallelly recreated with the separation of 240 µm to create a THz MIMO antenna, as illustrated in Fig.1(a). This antenna configuration exhibits strong mutual coupling among the ports of the MIMO and a poor reflection coefficient. The vector surface current distribution plot shows the mutual coupling among the interelement, as depicted in Fig.1(b).

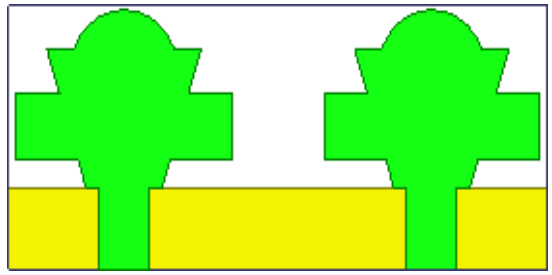

(a)

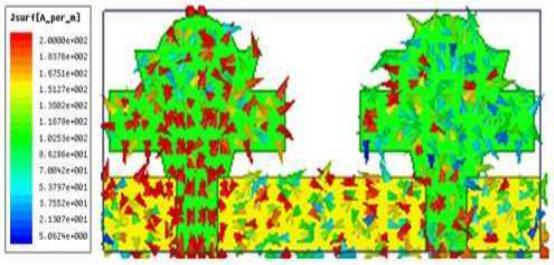

(b)

Fig.1. Two-port THz antenna without decoupling structure (a) THz MIMO antenna, (b) vector current distribution plot.

The antenna configuration is adjusted to increase the reflection coefficient and isolation of the THz MIMO antenna by integrating a hybrid decoupling structure consisting of a neutralization line (NL) onto the radiator and DGS. A horizontal stub of width 20 µm connects the two THz antennae and forms an NL. The NL generates the same magnitude of a field but is out of phase as that of the excited antenna element and helps decouple the coupling effect. On the contrary, DGS suppresses the field and does not allow it to reach the neighboring element by acting as band-stop characteristics. The proposed THz MIMO antenna operates in the frequency range of 0.87-1.9 THz, having isolation better than 22 dB across the impedance bandwidth of the antenna. The geometrical information of the proposed antenna is illustrated in Fig.2 and Table I.

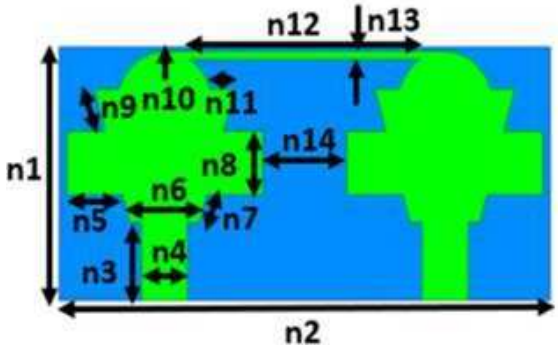

(a)

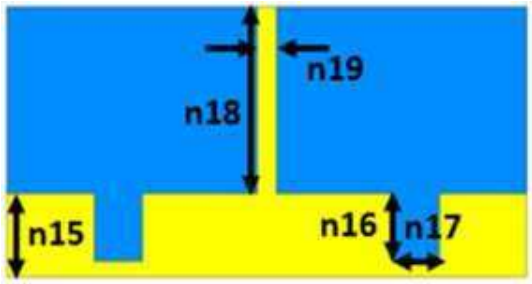

(b)

Fig.2. Proposed THz MIMO antenna (a) radiator, (b) ground plane.

Table I. Physical information of the THz MIMO antenna (µm)

n1	**n2**	**n3**	**n4**	**n5**	**n6**	**n7**	**n8**	**n9**	
600	1400	185	130	160	197	20	150	32	
n10	**n11**	**n12**	**n13**	**n14**	**n15**	**n16**	**n17**	**n18**	**n19**
140	69	800	20	240	185	150	130	415	130

The proposed THz MIMO antenna structure evolved through successive phases of antenna arrangement change with respect to the reflection and transmission coefficients curves, as shown in Fig.3. The ant 1 in Figure 3 has no decoupling structure and a decent reflection coefficient, but the isolation between the inter ports is quite poor. In the second stage, the antenna's ground plane is modified by embedding a verticle rectangular stub at the center of the ground plane, as depicted in ant 2 of Figure 3. This modification provides 1.2-1.8 THz operating frequency with isolation better than 30 dB. The antenna structure is adjusted by adding the NL onto the radiator to achieve a wider impedance bandwidth and effective isolation. The right position and form of the NL are critical in ensuring excellent isolation among the MIMO elements and are achieved by a series of iterations from ant 3 to ant 6, as in Fig.3(a). Figure 3(b) depicts the reflection and transmission coefficient curves for each individual stage. The proposed ant 6 THz MIMO operates at 0.87-1.9 THz and has isolation greater than 22 dB.

The proposed THz MIMO antenna's isolation is ensured by plotting the vector surface distribution plot at the resonant frequency of 1.3 THz. The highest current focused at the feedline, the center of the excited element, and onto the hybrid decoupling structure is shown in this plot. The neighboring element exhibits negligible field coupling, as illustrated in Fig.4.

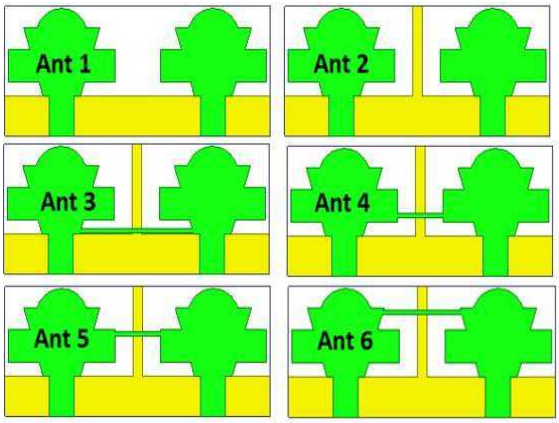

(a)

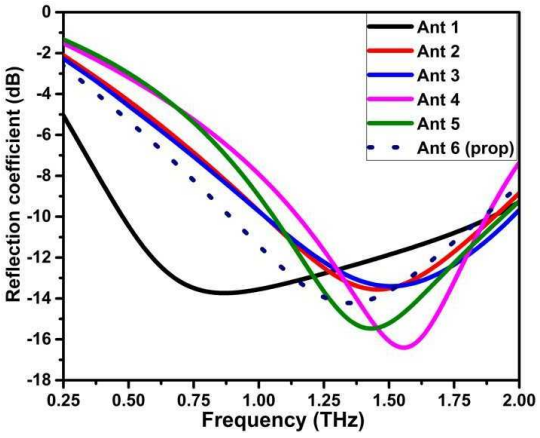

(b)

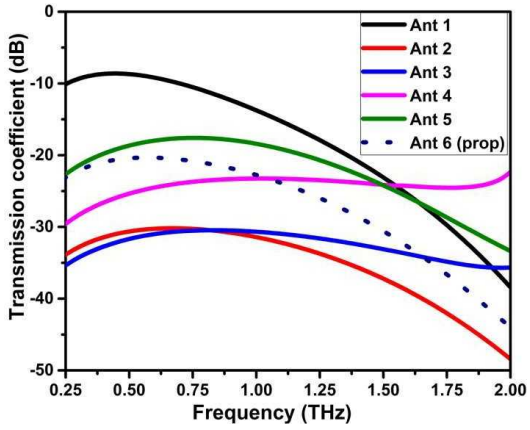

(c)

Fig.3. Evolution of the proposed THZ MIMO antenna configuration (a) antenna geometry evolution (b) reflection, and (c) transmission coefficient curves.

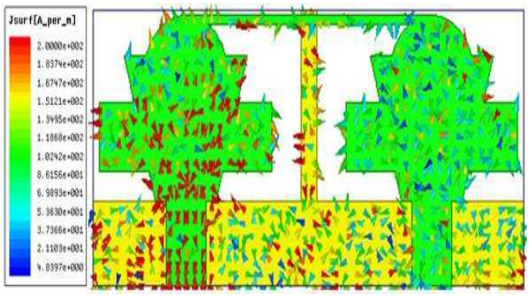

Fig.4. Vector surface current distribution plot at 1.35 THz.

III. Results and Discussions

The proposed THz MIMO antenna is designed on a polyimide substrate with a thickness of 20 µm and dielectric constant of 3.5 using ANSYS HFSS. The scattering parameters, radiation properties, and MIMO diversity features are examined for the proposed antenna.

The proposed THz MIMO antenna functions in the frequency range of 0.87-1.9 THz, and isolation between inert elements is greater than 22 dB at the antenna's working frequency, as shown in Fig.5. The hybrid decoupling structure aids in the realization of improved isolation in the given MIMO antenna.

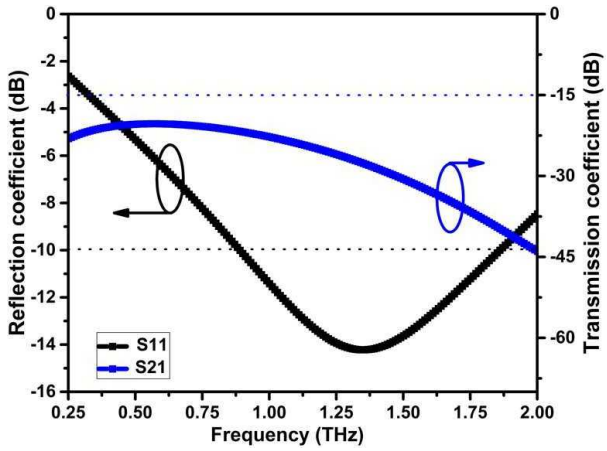

Fig.5. S-parameters of the THz MIMO antenna.

The proposed antenna's two-dimensional co and the cross-polarization radiation pattern are plotted in two XZ and YZ principal planes. The radiation pattern demonstrates the quasi-bidirectional and omnidirectional pattern in E and H-planes correspondingly, as depicted in Fig.6. The gain of the antenna at the resonant frequency of 1.3 THz is 1.65 dB, as represented in Fig.7.

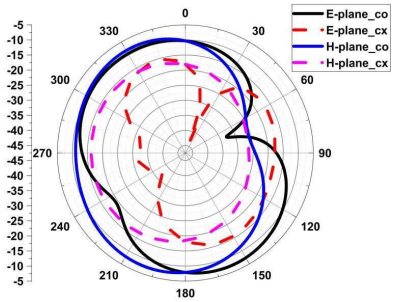

Fig.6. Radiation pattern at 1.35 THz frequency.

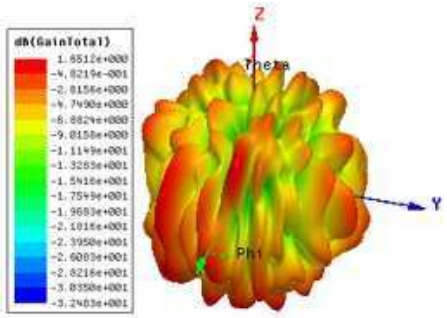

Fig.7. Gain of the proposed antenna at 1.35 THz.

The MIMO diversity features, such as the envelope correlation coefficient (ECC), describe the quantity of coupling among the inter elements of the MIMO antenna. The diversity gain (DG) defines the strength of the signal with reference to the interference. The DG is associated with the ECC. The total active reflection coefficient (TARC) specifies the MIMO antenna's total return loss. The mean effective gain (MEG) describes the antenna's capacity to receive electromagnetic radiation in a fading environment. The channel capacity loss (CCL), which specifies the maximum rate at which the data may be appropriately transferred, defines reliable communication. These MIMO diversity parameters are computed using the following equations (1-5). The diversity features of the proposed antenna are ECC <0.001, DG≈ 10 dB, TARC <-10 dB, CCL<0.2 bps/Hz, and MEG<-3 dB across the impedance bandwidth of the antenna as shown in Fig.8.

$$ECC = \frac{|S^*_{11} S_{12} + S^*_{21} S_{22}|^2}{(1 - |S_{11}|^2 - |S_{21}|^2)(1 - |S_{22}|^2 - |S_{12}|^2)} \quad (1)$$

$$DG = 10\sqrt{1 - ECC} \quad (2)$$

$$TARC = \sqrt{\frac{(S_{11} + S_{12})^2 + (S_{21} + S_{22})^2}{2}} \quad (3)$$

$$CCL = -log_2 \det(\alpha)^R \quad (4)$$

where α^R is the receiving antenna correlation matrix, for two element α^R is as follows

$$\alpha^R = \begin{vmatrix} \rho_{11} & \rho_{12} \\ \rho_{21} & \rho_{22} \end{vmatrix}$$

where $\rho_{ii} = 1 - |\sum_{n=1}^{N=2} S^*_{i,n} S_{n,i}|$ and $\rho_{ij} = -|\sum_{n=1}^{N=2} S^*_{i,n} S_{n,j}|$ for $i, j = 1, 2$.

$$MEG_i = 0.5\,(1 - \sum_{j=1}^{M} |S_{ij}|) \quad (5)$$

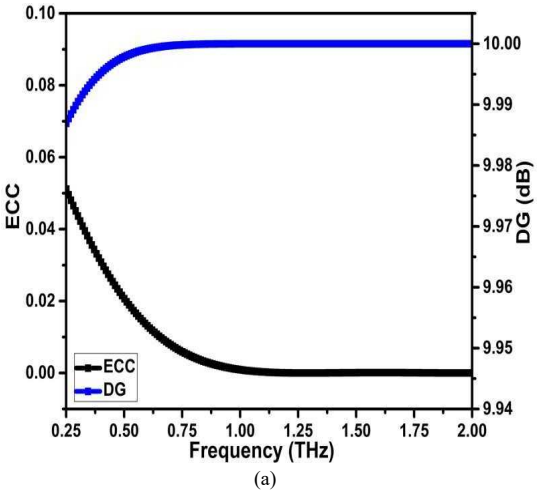

(a)

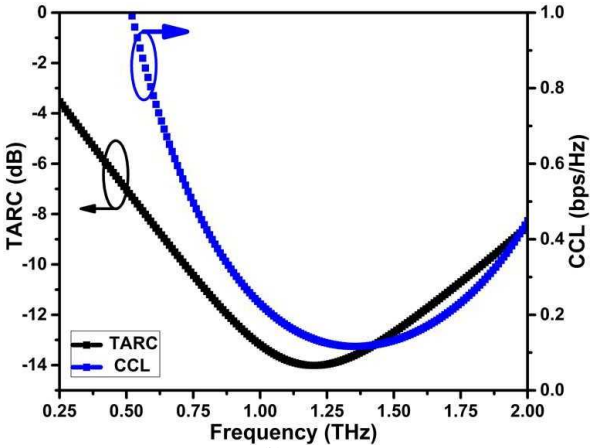

(b)

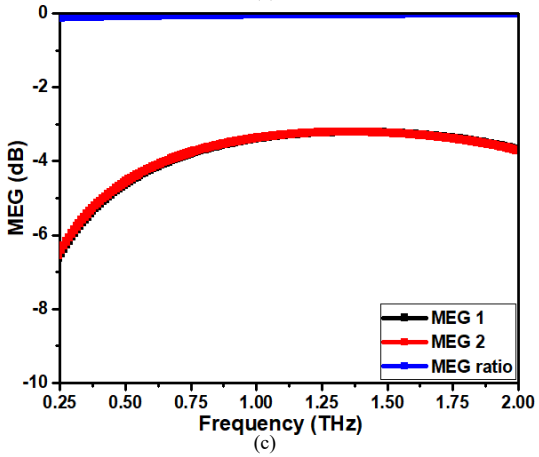

(c)

Fig.8. Diversity features (a) ECC and DG, (b) TARC and CCL, (c) MEG.

IV. COMPARATIVE ANALYSIS

The designed THz MIMO antenna performance is compared with similar existing designs in the literature, as listed in Table II and Table III. The proposed antenna is relatively large but has broader bandwidth and good isolation and diversity features.

TABLE II. COMPARATIVE ANALYSIS OF PROJECTED ANTENNA

Ref	Techniques used	Dimension (μm^3)	Bandwidth (THz)	Isolation (dB)
[16]	MTM loading	130×85×10	3.2-3.8	>25
[17]	MTM loading	84×84×10	1.1-1.7	25
[18]	MTM loading	380×380×10	1.1	>20
[19]	Parasitic elements	56×56×10	1.76	>50
Prop.	Hybrid structure	600×1400×20	0.87-1.9	>22

*-NA

TABLE III. COMPARATIVE ANALYSIS OF PROJECTED ANTENNA

Ref	ECC	DG	TARC	CCL	MEG
[16]	0.0002	≈ 10	-	0.006	-
[17]	0.01	-	-	-	-
[18]	-	-	-	-	-
[19]	0.008	≈ 10	-	-	-
Prop.	0.001	≈ 10	<-10	0.2	<-3

*-NA

V. CONCLUSION

The conventional rectangular patch antenna is modified and transformed into a Y-shaped radiator with a reduced ground plane to realize the THz operating frequency. The designed THz antenna is recreated parallelly to form the THz MIMO antenna operating in the frequency range of 0.87-1.9 THz with isolation better than 22 dB. The designed antenna is explored to the diversity features, and findings demonstrate that the antenna is appropriate for wireless communication across the operational frequency range.

REFERENCES

[1] P. Kumar, M. M. M. Pai, and T. Ali, "Metamaterials: New aspects in antenna design," Telecommun. Radio Eng., vol. 79, no. 16, pp. 1467–1478, 2020.

[2] P. Hillger, J. Grzyb, R. Jain, and U. R. Pfeiffer, "Terahertz imaging and sensing applications with silicon-based technologies," IEEE Trans. Terahertz Sci. Technol., vol. 9, no. 1, pp. 1–19, 2019.

[3] X. Yi et al., "Emerging terahertz integrated systems in silicon," IEEE Trans. Circuits Syst. I Regul. Pap., vol. 68, no. 9, pp. 3537–3550, 2021.

[4] J. M. Jornet and I. F. Akyildiz, "Graphene-based Plasmonic Nano-Antenna for Terahertz Band Communication in Nanonetworks," IEEE J. Sel. Areas Commun., vol. 31, no. 12, pp. 685–694, 2013.

[5] A. J. Fitzgerald, E. Berry, N. N. Zinovev, G. C. Walker, M. A. Smith, and J. M. Chamberlain, "An introduction to medical imaging with coherent terahertz frequency radiation," Phys. Med. Biol., vol. 47, no. 7, pp. R67-84, 2002.

[6] A. S. Dhillon, D. Mittal, and E. Sidhu, "THz rectangular microstrip patch antenna employing polyimide substrate for video rate imaging and homeland defence applications," Optik (Stuttg.), vol. 144, pp. 634–641, 2017.

[7] P. Kumar, T. Ali, S. Pathan, N. Kumar Shetty, Y. Bommenahalli Huchegowda, and Y. Nanjappa, "Design and analysis of ultra-wideband four-port MIMO antenna with DGS as decoupling structure for THz applications," Results in Optics, vol. 13, no. 100573, p. 100573, 2023.

[8] S. Poorgholam-Khanjari and F. B. Zarrabi, "Reconfigurable Vivaldi THz antenna based on graphene load as hyperbolic metamaterial for skin cancer spectroscopy," Opt. Commun., vol. 480, no. 126482, p. 126482, 2021.

[9] G. Geetharamani and T. Aathmanesan, "Split ring resonator inspired THz antenna for breast cancer detection," Opt. Laser Technol., vol. 126, no. 106111, p. 106111, 2020.

[10] G. Saxena, Y. K. Awasthi, and P. Jain, "High isolation and high gain super-wideband (0.33-10 THz) MIMO antenna for THz applications," Optik (Stuttg.), vol. 223, no. 165335, p. 165335, 2020.

[11] S. A. Khaleel, E. K. I. Hamad, N. O. Parchin, and M. B. Saleh, "MTM-inspired graphene-based THz MIMO antenna configurations using characteristic mode analysis for 6G/IoT applications," Electronics (Basel), vol. 11, no. 14, p. 2152, 2022.

[12] P. Das, A. K. Singh, and K. Mandal, "Metamaterial loaded highly isolated tunable polarisation diversity MIMO antennas for THz applications," Opt. Quantum Electron., vol. 54, no. 4, 2022.

[13] I. Aggarwal, S. Pandey, M. R. Tripathy, and A. Mittal, "A compact high gain metamaterial-based antenna for terahertz applications," J. Electron. Mater., vol. 51, no. 8, pp. 4589–4600, 2022.

[14] R. Singh, G. Varshney, "Isolation enhancement technique in a dual-band THz MIMO antenna with single radiator," Opt Quant Electron, vol. 55, no. 539, 2023.

[15] S.-E. Didi et al., "Study and design of the microstrip patch antenna operating at 120 GHz," in Terahertz Wireless Communication Components and System Technologies, Singapore: Springer Singapore, 2022, pp. 175–190.

[16] S. A. Khaleel, E. K. I. Hamad, N. O. Parchin, and M. B. Saleh, "MTM-inspired graphene-based THz MIMO antenna configurations using characteristic mode analysis for 6G/IoT applications," Electronics (Basel), vol. 11, no. 14, p. 2152, 2022.

[17] B. Zhang, J. M. Jornet, I. F. Akyildiz, and Z. P. Wu, "Mutual coupling reduction for ultra-dense multi-band plasmonic nano-antenna arrays using graphene-based frequency selective surface," IEEE Access, vol. 7, pp. 33214–33225, 2019

[18] P. Kumar, T. Ali, and M. M. Pai, "A compact highly isolated two-and four-port ultrawideband Multiple Input and Multiple Output antenna with Wireless LAN and X-band notch characteristics based on Defected Ground Structure," International Journal of Communication Systems, vol. 35, no. 17, 2022.

[19] M.F. Ali, R. Bhattacharya, and G. Varshney, "Tunable four-port MIMO/self-multiplexing THz graphene patch antenna with high isolation," Opt. Quantum Electron., vol. 54, no. 12, p.822, 2022.